THE JOURNAL OF BIOLOGICAL CHEMISTRY VOL. 287, NO. 15, pp. 11798–11809, April 6, 2012

Refinement of Structural Leads for Centrally Acting Oxime Reactivators of Phosphylated Cholinesterases*[S]

Received for publication, December 14, 2011, and in revised form, February 3, 2012 Published, JBC Papers in Press, February 16, 2012, DOI 10.1074/jbc.M111.333732

Zoran Radić[‡1], Rakesh K. Sit[§1], Zrinka Kovarik[¶], Suzana Berend[¶], Edzna Garcia[‡], Limin Zhang[‡], Gabriel Amitai[‖], Carol Green[**], Božica Radić[¶], Valery V. Fokin[§], K. Barry Sharpless[§], and Palmer Taylor[‡2]

*From the [‡]Skaggs School of Pharmacy and Pharmaceutical Sciences, University of California at San Diego, La Jolla, California 92093, the [§]Skaggs Institute for Chemical Biology, The Scripps Research Institute, La Jolla, California 92037, the [¶]Institute for Medical Research and Occupational Health, HR-10001 Zagreb, Croatia, the [‖]Department of Pharmacology, Israel Institute for Biological Research, Ness Ziona 74100, Israel, and **SRI International, Menlo Park, California 94025-3493*

Background: Contemporary oxime antidotes to organophosphate poisoning cannot penetrate CNS to reactivate inhibited acetylcholinesterase.
Results: Structural, *in vitro* optimization of ionizable hydroxyiminoacetamido amine acetylcholinesterase reactivators produced superior antidotal responses for VX-, sarin-, paraoxon-, and tabun-exposed mice.
Conclusion: Ionizable hydroxyiminoacetamido amines are promising centrally active acetylcholinesterase reactivators.
Significance: A mechanism-based iterative refinement of acetylcholinesterase reactivation kinetics coupled with pharmacokinetic analyses yields efficient CNS penetrating antidotes.

We present a systematic structural optimization of uncharged but ionizable *N*-substituted 2-hydroxyiminoacetamido alkylamine reactivators of phosphylated human acetylcholinesterase (hAChE) intended to catalyze the hydrolysis of organophosphate (OP)-inhibited hAChE in the CNS. Starting with the initial lead oxime RS41A identified in our earlier study and extending to the azepine analog RS194B, reactivation rates for OP-hAChE conjugates formed by sarin, cyclosarin, VX, paraoxon, and tabun are enhanced severalfold *in vitro*. To analyze the mechanism of intrinsic reactivation of the OP-AChE conjugate and penetration of the blood-brain barrier, the pH dependence of the oxime and amine ionizing groups of the compounds and their nucleophilic potential were examined by UV-visible spectroscopy, ^{1}H NMR, and oximolysis rates for acetylthiocholine and phosphoester hydrolysis. Oximolysis rates were compared in solution and on AChE conjugates and analyzed in terms of the ionization states for reactivation of the OP-conjugated AChE. In addition, toxicity and pharmacokinetic studies in mice show significantly improved CNS penetration and retention for RS194B when compared with RS41A. The enhanced intrinsic reactivity against the OP-AChE target combined with favorable pharmacokinetic properties resulted in great improvement of antidotal properties of RS194B compared with RS41A and the standard peripherally active oxime, 2-pyridinealdoxime methiodide. Improvement was particularly noticeable when pretreatment of mice with RS194B before OP exposure was combined with RS194B reactivation therapy after the OP insult.

A recent spur of interest in centrally acting reactivators of organophosphate (OP)[3] inhibited acetylcholinesterase (AChE) (1–6) reflects a compelling need for antidotal therapy capable of efficient reinstatement of CNS AChE activity in OP-intoxicated individuals. Exposure to uncharged, lipophilic OPs from both pesticide and nerve agents leads to inhibition of peripheral and CNS AChE within minutes of exposure due to rapid OP diffusion through biological membranes of exposed individuals (7). However, attention has been accorded primarily to the development of largely cationic reactivator antidotes in line with recognition that quaternary ammonium ligands have a clear preference for association with predominantly aromatic active center gorge of AChE (8–14). When administered *in vivo*, quaternary oxime reactivators largely remain in blood and peripheral tissue incapable of crossing the blood-brain barrier and reactivating OP-inhibited brain AChE (15). An ideal centrally acting reactivator should thus combine the properties of efficient reactivation and blood brain barrier penetration. Our initial approach was to develop a library of uncharged oxime reactivators amenable to protonation (1) and identify a lead structure. A reactivator, RS41A (Table 1), comparable in its *in vitro* reactivating potency to standard pyridinium oxime reactivator 2PAM, was selected from a large synthetic library.

In this study we describe systematic variations of RS41A structure and a detailed evaluation of associated reactivating properties leading to several enhanced reactivators culminating in the severalfold improved azepine analog RS194B. By virtue of enhanced association with OP-hAChE conjugates, RS194B showed substantially improved *in vitro* reactivation kinetics compared with the initial lead RS41A. Moreover, the low tox-

* This work was supported, in whole or in part, by the CounterACT Program, National Institutes of Health Office of the Director, and National Institutes of Health Grant U01 NS058046 from NINDS.
[S] This article contains supplemental Figs. S2–S6 and Tables S1–S6.
[1] Both authors contributed equally to this work.
[2] To whom correspondence should be addressed: SSPPS, UCSD, 9500 Gilman Drive, La Jolla, CA 92093-0657. Tel.: 858-534-44028; Fax: 858-534-8248; E-mail: pwtaylor@ucsd.edu.

[3] The abbreviations used are: OP, organophosphate; AChE, acetylcholinesterase; hAChE, human AChE; ATCh, acetylthiocholine; 2PAM, 2-pyridinealdoxime methiodide; MINA, monoisonitrosoacetone; DAM, 2,3-butanedione monoxime; PI, protective index; Flu-MP, fluorescent methylphosphonates; i.m., intramuscular; VX, *O*-ethyl *S*-[2-(diisopropylamino)ethyl] methylphosphonothioate.

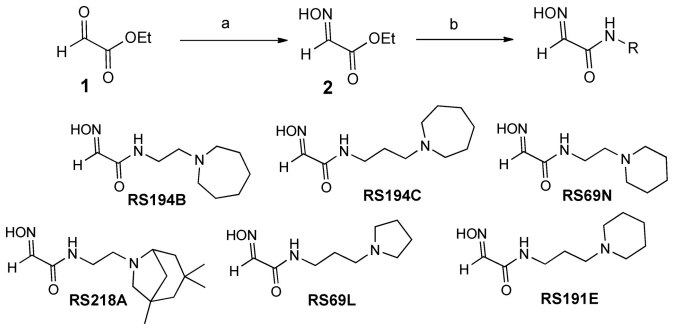

Reagents: (a) $NH_2OH{\cdot}HCl$, Et_3N, CH_3CN, H_2O, rt; (b) RNH_2, C_2H_5OH, 50 °C

SCHEME 1

icity of RS194B in the mouse animal model in combination with its enhanced intrinsic reactivity results in substantial improvement of its therapeutic properties compared with RS41A and the standard oxime, 2PAM. The improvement was particularly noticeable when pretreatment of mice with RS194B before OP exposure was combined with RS194B reactivation therapy after the OP insult. We describe here the mechanistic basis for this enhancement in terms of the intrinsic reaction constants and pharmacokinetic profiles.

MATERIALS AND METHODS

Enzyme—Highly purified monomeric hAChE was prepared as described earlier (1, 16).

Organophosphates—Low toxicity, nonvolatile fluorescent methylphosphonates (Flu-MPs) (17) were used in *in vitro* experiments as analogues of nerve agents sarin, cyclosarin, and VX. The Flu-MPs differ from actual nerve agent OPs only by the structure of their respective leaving groups. Inhibition of hAChE by Flu-MPs results in OP-hAChE covalent conjugates identical to the ones formed upon inhibition with the corresponding volatile OPs. Paraoxon was purchased from Sigma. Nerve agent OPs tabun, VX, sarin, and soman used in *in vivo* experiments were purchased from NC Laboratory (Spiez, Switzerland).

Oximes—2-Pyridinealdoxime methiodide (2PAM), monoisonitrosoacetone (MINA), and 2,3-butanedione monoxime (DAM) were purchased from Sigma.

Preparation of Novel Oximes—*N*-Substituted 2-hydroxyiminoacetamides RS194B, RS194C, RS69N, RS218A, RS69L, and RS191E were prepared from ethyl glyoxylate (*1*) in two steps (Scheme 1). Condensation with hydroxylamine provided ethyl glyoxylate oxime (*2*) followed by subsequent amidation with the corresponding primary amine.

In Vitro Oxime Reactivation Assays—hAChE activities were measured using a spectrophotometric assay (18) at 25 °C in 0.1 M sodium phosphate buffer, pH 7.4, containing 0.01% BSA and 1.0 mM substrate acetylthiocholine (ATCh). OP-hAChE conjugates were prepared, and oxime reactivation was performed (at 37 °C in 0.1 M sodium phosphate buffer, pH 7.4, containing 0.01% BSA) as described earlier (1, 16). The first order reactivation rate constant (k_{obs}) for each oxime + OP conjugate combination was calculated by nonlinear regression (19). The dependence of reactivation rates on oxime concentrations and determination of maximal reactivation rate constant k_2, Michaelis-Menten type constant K_{ox}, and the overall second order reactivation rate constant k_r were conducted as previously described (19). The pH dependence of oxime reactivation of AChE was performed in 0.1 M phosphate buffers pH 6.4, 7.4, or 8.4 containing 0.01% BSA.

Oxime pK_a Determinations—Protonation of ionizable groups in oximes was monitored either using UV-visible spectrophotometry or by NMR spectrometry. A series of 20 mM phosphate-pyrophosphate buffers pH 5.0, 6.0, 7.0, 8.0, 8.5, 9.0, 9.5, 10, 10.5, and 11 (containing 0.1 M NaCl) were prepared in either H_2O or D_2O. For D_2O buffers, pD values were determined by correcting the pH reading by +0.4 pH units (*cf.* Ref. 20). UV spectra of oximes between 220- and 320-nm wavelengths were recorded on Cary 1E (Varian) UV-visible spectrophotometer at the above pH values, and absorbance at 270 nm ($A_{270\ nm}$) was plotted as a function of pH yielding pK_a values by nonlinear regression of Equation 1.

$$A_{270\ nm} = A^{max}_{270\ nm}/(1 + [H^+]/K_a) \qquad \text{(Eq. 1)}$$

^{1}H NMR spectra recorded on Bruker DRX-500 (Bruker, USA) spectrometer in 20 mM phosphate-pyrophosphate D_2O buffers pH 5.0, 6.0, 7.0, 8.0, 8.5, 9.0, 9.5, and 10 (containing 0.1 M NaCl) were overlaid and aligned using benzene as an external standard placed in a separate capillary tube within the NMR sample probe. Two-dimensional ^{1}H,^{1}H double-quantum filtered COSY spectra were recorded on a Bruker DRX-600 spectrometer.

Computational Molecular Modeling—Interactions of oximes RS41A and RS194B within the active center gorge of VX-inhibited hAChE were studied for the reversible complex and for the trigonal bipyramidal intermediate for the reactivation step using a simulated annealing molecular dynamics approach (21). Covalent conjugates of hAChE ethylmethylphosphonylated at the active Ser-203 were generated by pasting ethylmethylphosphonylated Ser-203 of mouse AChE structure (PDB 2JGH) into the native WT hAChE structure (PDB 3LII) and subsequent semiempirical quantum mechanical adjustment of partial charges by InsightII suite (Accelrys, San Diego, CA). All water molecules were removed from the PDB structures, and a dielectric constant of four was used in calculation to mimic the interior of the hAChE active center gorge. In calculations for formation of the reversible complex, distances between oximate oxygen and the P atom of the VX conjugate were flexibly constrained to a distance between 0 and 3.00 Å. In trigonal bipyramidal intermediate calculations, the oximate oxygen was covalently linked to the P atom rehybridized to pentacoordinate geometry (21). Ten calculations were made for each oxime at both the reversible complex and trigonal bipyramidal intermediate steps allowing the oxime molecule and hAChE residues 72, 124, 286, 297, 341, and VX-conjugated Ser-203 to rotate freely, whereas all other enzyme side chains were fixed.

Acute Oxime Toxicity and Oxime Treatment of OP-exposed Mice—Male CD-1 mice (25–30 g body weight) were purchased from Rudjer Bošković Institute, Zagreb, Croatia. Mice were fed on a standard diet, had free access to water, and were kept in Macrolone cages at 21 °C, exchanging light and dark cycles every 12 h. For the experimental sequence, mice were divided

into groups of four. The mice were treated in accord with the approval of the Ethical Committee of the Institute for Medical Research and Occupational Health in Zagreb, Croatia.

Acute intramuscular (i.m.) toxicity (LD_{50}) was based upon 24-h mortality rates calculated according to Thompson (22) and Weil (23). Each LD_{50} was evaluated from the results obtained with four to six doses of a given oxime (dissolved in water plus a minute amount of HCl to form the corresponding hydrochloride salt).

Antidotal activity against OP poisoning was tested by giving male CD-1 mice the studied oximes i.m. (at the specified dose) together with atropine sulfate (10 mg/kg) 1 min after subcutaneous OP administration (24, 25). Stock solutions of nerve agents were prepared in isopropyl alcohol or in propylene glycol. Further dilutions were made in saline immediately before use. Alternatively, mice were pretreated i.m. with oximes (at specified dose but without atropine) 5 or 15 min before subcutaneous OP administration. The combination of pretreatment and antidotal therapy was performed by i.m. pretreatment with oxime 15 min before subcutaneous OP administration followed by i.m. administration of oxime (dissolved in 5 mg/ml atropine sulfate) 1 min after the OP exposure.

The antidotal efficacy of oximes was expressed as protective index (PI) with 95% confidence limits and the maximal dose of OP. The PI was the ratio of LD_{50} between OP with antidote and OP given alone. The maximal dose of organophosphate was the highest multiple of the OP LD_{50}, which was fully counteracted by the oximes.

Oxime Pharmacokinetics in Mice—Female CD-1 mice 4–8 weeks old (22–34 g of body weight) were purchased from Harlan (Livermore, CA). Mice were fed Purina Certified Rodent Chow #5002. Food and purified water were provided *ad libitum*. Mice were kept in hanging polycarbonate cages at 21–23 °C, exchanging light and dark cycles every 12 h. General procedures for animal care and housing were in accordance with the National Research Council Guide for the Care and Use of Laboratory Animals (1996) and the Animal Welfare Standards incorporated in 9 CFR Part 3, 1991.

For experiments mice were divided into groups of three. In the pharmacokinetic studies, 80 mg/kg RS194B or 30 mg/kg RS41A oxime was administered i.m. as a single dose in the absence of OP. Three animals were injected for every time point analyzed. Brain and plasma were collected at each time point. Blood (~300 μl) was collected from the retro-orbital sinus of mice under isoflurane anesthesia into tubes containing EDTA, processed to plasma within 30 min of collection, and then stored frozen at ≤−80 °C (± 10 °C).

Brains were collected and analyzed individually at each time point. Brain weight was documented for each animal before storage on dry ice. Brains were stored at ≤−80 °C (± 10 °C) until analysis. Concentration of the oxime in body compartments was determined by LC-MS using multiple reaction monitoring electrospray ionization detection in positive ion mode.

RESULTS

Systematic Variations of RS41A Structure—Our recent characterization (1) of a library of 135 uncharged, structurally diverse oximes revealed hydroxyimino acetamido amines as efficient reactivators of OP-hAChE conjugates. In particular, the selected lead structure RS41A appeared similar in reactivation potency to the standard reference oxime 2PAM. With the aim of better understanding structure/activity relationships of the hydroxyimino acetamido alkylamine reactivators and specifically improving RS41A reactivation properties, we synthesized new reactivators by systematically modifying structure (Table 1). In analyzing the alkylamine substituent attached to the 2-hydroxyimino acetamide, we distinguished two elements: the heterocycle "handle" and an intervening methylene "linker." Starting with the 2-hydroxyimino acetamido amine RS157A (no linker), ethyl, *n*-propyl, and *n*-butyl linkers were introduced along with primary amine, dimethylamine, pyrrolidine, piperidine, azepane, azocane, and bridged, polycyclic handles. Small amine and dimethylamine handles did not prove helpful, resulting in largely inactive reactivators (the last four compounds in Table 1) irrespective of the associated linker length. Both ethyl and propyl linkers proved effective. Of four pairs of compounds containing an identical handle, the ethyl linker proved more efficient in two pairs (RS194B *versus* RS194C and RS41A *versus* RS69L) and the propyl linker in the other two pairs (RS251B *versus* RS251A and RS191E *versus* RS69N). Overall, the most effective reactivators were RS194B and RS191E where RS41A structure was extended either through linker or handle size, but combining both longer linker and larger handle (as in compound RS194C) was not productive. The further increase in handle size to either an eight-membered azocane ring (RS251A and RS251B), bridged azepane (RS218A), or seven membered rings (RS2–57B) or by making it bicyclic yielded a respectable but not superior reactivator. Analysis of molecular volumes and solvent-accessible surface areas for the N substituents (Table 1) suggests that the most efficient reactivators fall in the group of those having volume/surface area ratio between 0.87 and 0.92, suggesting that for this series of relatively similar compounds, a more spheroid rather than planar shape appears more productive. Intrinsic reactivities of all 16 compounds from Table 1 reflected in their measured rates of ATCh oximolysis as well as the calculated percents of respective oximate anions were similar, emphasizing the importance of the shape and charge distribution for the productive interaction with OP-AChE conjugates leading to recovery of enzyme activity.

Reactivation Kinetics of Selected Oximes in Vitro—To distinguish whether molecular recognition or intrinsic chemical reactivity of RS41A was dominant in influencing overall reactivation potency, we analyzed reactivation kinetics of seven leading congeners of RS41A and three reference oximes, 2PAM, MINA, and DAM, and determined their individual reactivation constants k_2 and K_{ox} (Table 2; Fig. 1). In the analysis we assume that K_{ox} mainly reflects initial reversible interaction of oxime reactivator with an OP-hAChE conjugate, whereas k_2 reflects the interaction of the reactivating oxime or oximate nucleophile with the phosphate moiety of the OP-conjugated hAChE in leading to the trigonal bipyramidal intermediate for reactivation. A pairwise comparison of six reactivators containing the identical handle and different methylene linkers reveals that trigonal bipyramidal intermediate for the oximate reaction prefers a shorter linker, whereas the initial reversible binding

TABLE 1

Structures and initial screen of relative rate constants (k_{obs}) for OP-hAChE reactivation of selected uncharged reactivators (0.67 mM) in comparison to cationic pyridinium aldoxime 2PAM

Nonenzymic oximolysis rates of ATCh (1 mM) by 1.0 mM oximes and calculated percentages of oximate anion and neutral species at pH 7.4 are also given as well as volume and surface area of R in the general oxime formula HO=NCHC(O)NH-R. Experiments were performed in duplicate at 37 °C in 0.10 M phosphate buffer, pH 7.4.

Oxime	Oxime structure	k_{obs} (relative to 2PAM)*					Oximolysis (dA/min)	% Oximate @ pH 7.4	% Neutral @ pH 7.4	R Volume (Å^3)	R Area (Å^2)
		Ave	POX	Sarin	CS	VX					
RS2-31B	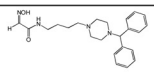	1.1	0.24	0.85	2.4	0.95	0.099	0.25	4.4	299	324
RS189A	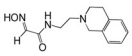	1.4	0.11	1.0	2.6	1.7	0.124	0.21	26	156	180
RS2-57B	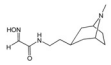	0.16	0.084	0.11	0.19	0.26	0.181	0.23	0.17	161	173
RS218A	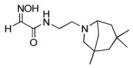	0.91	0.23	1.1	1.5	0.80	0.128	0.35	1.0	196	199
RS251B	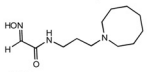	0.82	0.34	1.0	1.2	0.74	0.074	0.13	0.31	173	188
RS251A	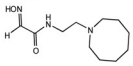	0.55	0.11	0.69	0.83	0.56	0.108	0.26	2.2	156	170
RS194C	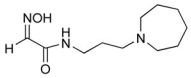	0.58	0.37	0.88	0.39	0.68	0.120	0.30	0.49	157	174
RS194B	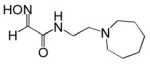	2.5	0.53	3.1	3.6	2.7	0.128	0.25	3.5	139	156
RS191E	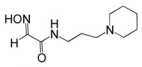	2.0	0.39	1.6	3.5	2.7	0.126	0.30	1.4	140	161
RS69N	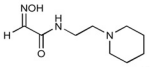	0.53	0.200	0.400	0.500	1.0	0.135	0.22	9.5	123	143
RS69L	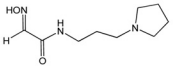	0.55	0.16	0.80	0.24	1.0	0.119	0.30	1.0	124	148
RS41A	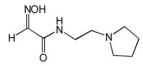	0.88	0.10	1.0	1.3	1.1	0.109	0.20	7.0	107	130
RS41B	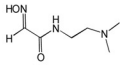	0.26	0.073	0.21	0.20	0.56	0.127	0.21	7.0	83	107
RS160C	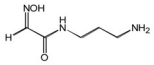	0.091	0.052	0.030	0.18	0.10	0.117	0.27	0.43	69	94
RS157B	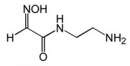	0.010	0.010	0.010	0.010	0.010	0.078	0.41	1.7	52	76
RS157A	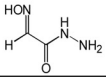	0.010	0.010	0.010	0.010	0.010	0.128	0.5	99.5	19	37

* The approximate k_{obs} values determined for 0.67 mM 2PAM were: 0.087 min^{-1} (for paraxon (POX)), 0.16 min^{-1} (for sarin), 0.025 min^{-1} (for cyclosarin (CS)), 0.15 min^{-1} (for VX). The experimental uncertainty of individual constant determination in the screen was about 50%.

within the gorge appears frequently better for the propyl derivatives. Indeed, k_2 constants for the pairs RS194B *versus* RS194C, RS69N *versus* RS191E, and RS41A *versus* RS69L were frequently larger in respective ethyl derivatives, whereas K_{ox} constants appeared smaller in respective propyl derivatives, indicating stronger initial reversible interaction between an oxime and OP-hAChE. On the other hand, increases in the handle size from pyrrolidine to piperidine and azepane rings resulted primarily in smaller K_{ox} values, whereas k_2 constants remained largely unchanged. One could thus conclude that enhancement of reactivation rates observed for RS194B *versus* initial lead RS41A results primarily from improved molecular recognition while preserving ability to form productive trigonal bipyramidal intermediate adducts. In further increasing size of handle from azepane to substituted tropane (RS194B to RS218A), a similar trend of lowering K_{ox} can be observed for paraoxon and sarin conjugates. However, due to simultaneous loss of reaction efficiency (reflected in reduced k_2 constants), the overall reactivation efficiency of RS218A was not greater than that of RS194B. Hence, RS194B oxime, an azepane analog of the initial lead RS41A, appears as a severalfold better reactivator and significantly superior to the reference α-ketoximes, DAM and MINA, primarily due to enhanced molecular recognition of OP-hAChE conjugates.

pK_a Determinations for Lead Oximes—The initial lead RS41A and the best uncharged reactivator RS194B include at

TABLE 2

Kinetic constants for reactivation of paraoxon-, sarin-, cyclosarin-, VX- and tabun-hAChE conjugates by principal uncharged lead oxime RS194B initial lead RS41A, several oximes leading from RS41A to RS194B, and reference oximes 2PAM, MINA, and DAM

Maximal reactivation rate constant (k_2, min^{-1}), apparent dissociation constant of [oxime · OP-hAChE conjugate] reversible complex (K_{ox}, mM), and overall second order reactivation rate constant (k_r, M^{-1} min^{-1}) were determined from reactivation curves as presented in Fig. 2. All constants were determined from triplicate experiments. S.E. of determined kinetic constants were typically less than 30% that of the mean.

Oxime	Oxime structure	Paraoxon			Sarin			Cyclosarin			VX			Tabun		
		k_2	K_{ox}	k_r	k_2	K_{ox}	k_r	k_2	K_{ox}	k_r	k_2	K_{ox}	k_r	k_2	K_{ox}	k_r
RS194B	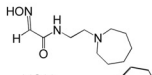	0.38	7.4	51	2.5	1.9	1300	0.88	3.9	230	3.1	2.1	16000	0.0018	1.8	1.0
RS194C	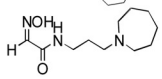	0.11	2.9	38	1.5	1.1	1400	0.90	4.3	210	1.9	2.4	790	n.d.	n.d.	n.d.
RS69N	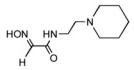	> 0.7	>50	13	2.2	2.2	1000	1.4	9.4	150	2.7	3.0	900	n.d.	n.d.	n.d.
RS218A	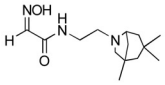	0.16	2.2	73	0.84	0.83	1000	0.53	5.4	98	1.3	2.2	590	n.d.	n.d.	n.d.
RS69L	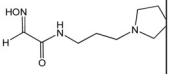	0.08	3.0	27	1.8	1.9	950	1.1	10	110	3.4	7.9	430	n.d.	n.d.	n.d.
RS41A	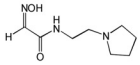	0.15	4.3	35	3.7	11	340	1.9	21	90	3.1	4.6	670	0.00082	3.6	0.22
RS191E	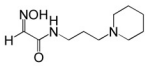	0.048	2.0	24	1.3	2.2	590	0.72	4.4	160	1.4	5.8	240	n.d.	n.d.	n.d.
RS186B	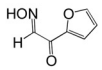	0.31	9.1	39	0.84	7.8	110	0.72	15	48	0.36	2.7	130	n.d.	n.d.	n.d.
MINA	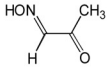	> 0.20	>20	8.4	1.6	14	120	1.2	16	75	>0.7	>6.0	110	-	-	0.039
DAM	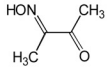	0.027	46	0.58	0.13	88	1.5	>0.30	>100	2.5	0.20	>100	1.7	-	-	0.0038
2PAM		0.27	1.8	150	1.1	0.34	3200	0.73	6.6	110	0.65	0.25	2600	0.0058	1.5	3.8

least two groups ionizable in the physiologically relevant pH range, affecting their reactivation potencies. Deprotonation of the oxime group is assumed to be essential for the oxime nucleophilic reactivity, whereas protonation of the handle ring nitrogen (azepane or pyrrolidine) should improve molecular recognition of a largely aromatic and partly anionic active center gorge of OP-hAChE adducts. Our goal was, therefore, to determine pK_a values of both ionizable groups for both RS41A and RS194B oximes. Initially UV-visible spectroscopy was used to record change in UV spectra of both oximes in the pH range 1–13 (Fig. 2). The increase in absorbance of both compounds at 270 nm results from deprotonation of the oxime hydroxyl, enabling us to determine a common pK_a value of 8.8 for both compounds (Fig. 2; Table 3).

Ionization states of the lead reactivator RS194B and the reference oxime 2PAM were studied in more detail using ^{1}H NMR spectrometry in D_2O medium (supplemental Figs. S1 and S2 and Fig. 3). We focused on position and appearance of three peaks in the RS194B spectrum (supplemental Fig. S1), the amido H peak present at ~7.65 ppm at pH 7.0, and two triplets coming from protons surrounding the azepane nitrogen and appearing at ~3.37 ppm and ~3.73 ppm at pH 7.0. Peak assignments were confirmed using the double-quantum filtered COSY spectra (supplemental Fig. 1*B*). Due to dissociation of the proton or deuteron, all three peaks shift to higher field at higher pH. The singlet at ~7.65 ppm shifts slightly to ~7.59 ppm at pH 10 (Fig. 3*A*). The triplet at ~3.38 ppm shifts slightly to ~3.28 ppm at pH 10 and becomes a complex multiplet (Fig. 3*B*), whereas the triplet at 3.73 ppm shifts to 3.68 ppm (Fig. 3*C*). Plotting the change of chemical shift in D_2O as a function of pH yields three pK_a values: 9.1 (equivalent to 9.1 – 0.5 = 8.6 in H_2O (27)) for loss of the imino hydrogen and pK_a values 9.3 (8.8 in H_2O) and 9.2 (8.7 in H_2O) for the azepane and pyrrolidine protons on the nitrogens (Fig. 3, *D*, *E*, and *F*; Table 3). Both ionizable groups should be largely protonated at the physiological pH of 7.4, thus rendering a cation dominant over the neutral, zwitterion, and anionic species.

In the ^{1}H NMR spectrum of 2PAM in D_2O, both the aldoxime CH peak and peaks of all aromatic protons shift simultaneously as a function of pH (supplemental Fig. S2). As expected, only the *N*-methyl peak at 2.8 ppm did not shift (data not shown). This indicates that the ionization state of the oxime group affects delocalization of aromatic system of 2PAM. This may influence the π-orbital interactions between the pyridinium ring and aromatic residues in the AChE gorge and consequently binding orientation of the reactivator. Analysis of pH-

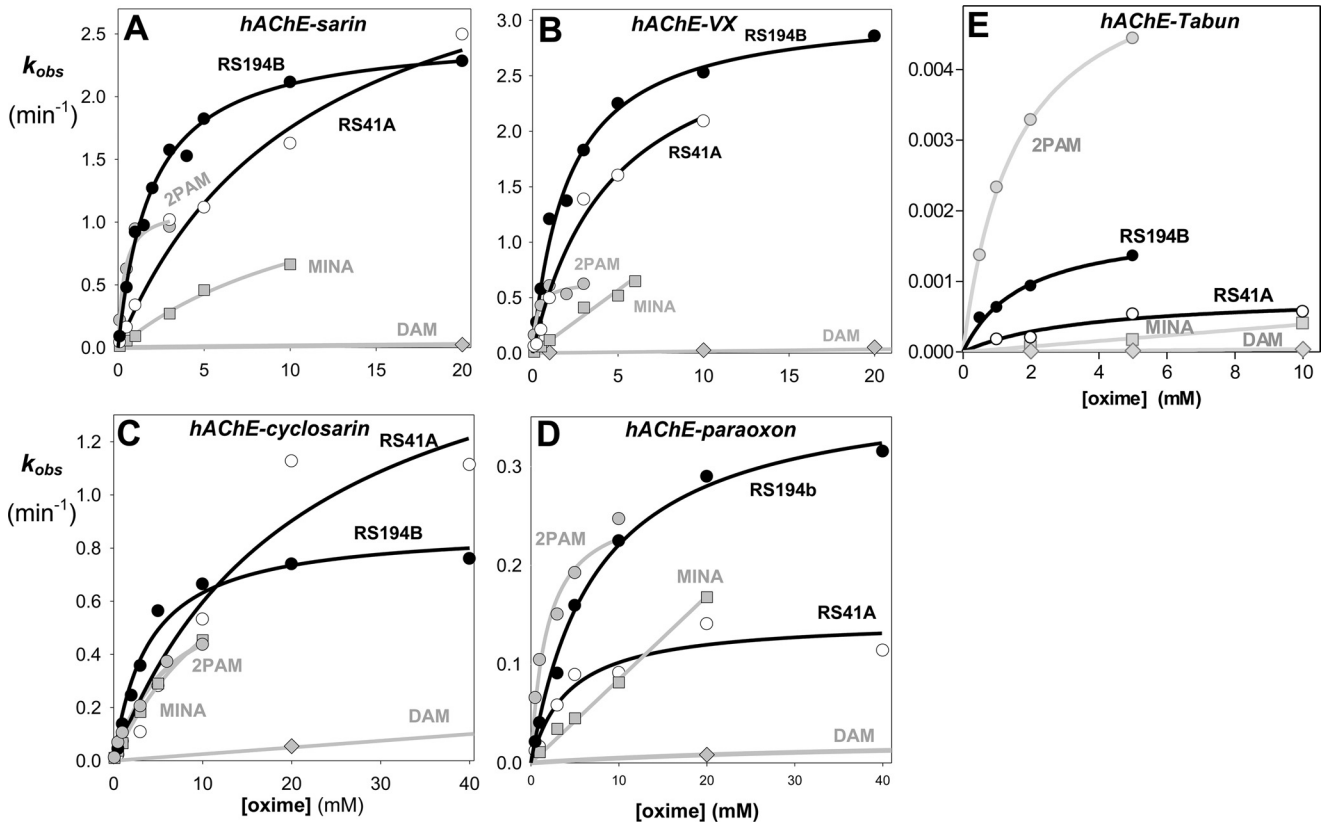

FIGURE 1. **Concentration dependence of oxime reactivation of sarin (*A*)-, VX (*B*)-, cyclosarin (*C*)-, paraoxon (*D*)-, and tabun (*E*)-inhibited (conjugated) hAChE.** Dependence for the lead oxime RS194B (*black circle*) and the initial lead RS41A (*open circle*) compared with reference uncharged (DAM (*gray diamond*) and MINA (*gray square*)) and cationic (2PAM (*gray square*) oximes (measured at 37 °C in 0.10 M phosphate buffer pH 7.4).

induced shifts of both the amido H peak (8.70 ppm at pH 7.0; supplemental Fig. S2*C*) and the doublet of aromatic proton at position 6 (8.75 ppm at pH 7.0; supplemental Fig. S2*D*) reveal a D_2O pK_a value of 8.6 (8.1 in H_2O) for the oxime group ionization (supplemental Fig. S2, *E* and *F*; Table 3).

pH Dependence of Oxime Nucleophilicity—The rates of oxime-induced hydrolysis (oximolysis) of ATCh and Flu-MP analog of VX measured spectrophotometrically and spectrofluorometrically were considered to be a measure of nucleophilic reactivity of an oxime. The pH dependence of ATCh oximolysis by RS41A, RS194B, and 2PAM revealed respective pK_a values of 9.0, 9.0, and 8.0 (supplemental Fig. S3) and pK_a values of 8.9, 8.7, and 8.1 for VX Flu-MP oximolysis (supplemental Fig. S4), consistent with UV and ^{1}H NMR-based pK_a determinations (Table 3). As expected, maximal oxime nucleophilicity was higher in oximates with higher pK_a values. However, at pH 7.4, the oxime-oximate pK_a comes into play where 2-PAM would have a greater nucleophilic capacity because of the greater fraction of oximate species.

pH Dependence of Reactivation Kinetics for Lead Oximes—Reactivation of VX-hAChE conjugate by RS41A and RS194B oximes as well as by RS186B and 2PAM measured in 0.1 M phosphate buffers at pH 6.4, 7.4, and 8.4 reveals no systematic changes of the overall reaction rate (reflected in k_r constant) (Table 4), whereas the nucleophilic first order reactivation rate constant k_2 did show a small increase with pH for all oximes. Consistent with its lowest pK_a value, the increase in k_2 was largest for 2PAM. However, although molecular recognition of 2PAM, reflected in K_{ox} constant, increased at lower pH, it did not change appreciably for the other two oximes. Thus, the protonated forms of both RS194B and RS41A oximes that dominate in large ratios at pH 6.4 as well as pH 7.4 with amine pK_a values around 8.9 (Table 3) did not bind to VX-hAChE conjugate as well as cationic 2PAM. The presence of a zwitterionic species at pH 8.4 (more than 50% of all forms for 2PAM and less than 50% for RS oximes) did not improve binding of RS oximes, whereas it slightly compromised binding of 2PAM (Table 4; Fig. 4).

Acute Oxime Toxicity and Oxime Treatment of OP-exposed Mice—The acute i.m. toxicity for mice of RS41A and in particular the lead reactivator RS194B was found to be relatively low (Table 5). Both oximes were less toxic than standard reference oxime 2PAM (LD_{50} = 106 mg/kg), whereas RS194B was similarly toxic as HI-6 (LD_{50} = 450 mg/kg) (data not shown), known as the least toxic standard oxime antidote.

OP-exposed mice treated with 125 mg/kg RS194B (a dose roughly equivalent to 25% of its LD_{50}) recovered significantly better from OP exposure than mice treated with an equivalent dose of RS41A and notably better than animals treated with 2PAM, with paraoxon-exposed mice being an exception (Table 5). Treatment of VX-exposed mice with lower RS194B doses equivalent to 10% of its LD_{50} (50 mg/kg) and 5% of its LD_{50} (25 mg/kg) yielded significant animal protection comparable with or better than 25% LD_{50} dose treatment by 2PAM, emphasizing the unique therapeutic efficacy of RS194B oxime (Table 6).

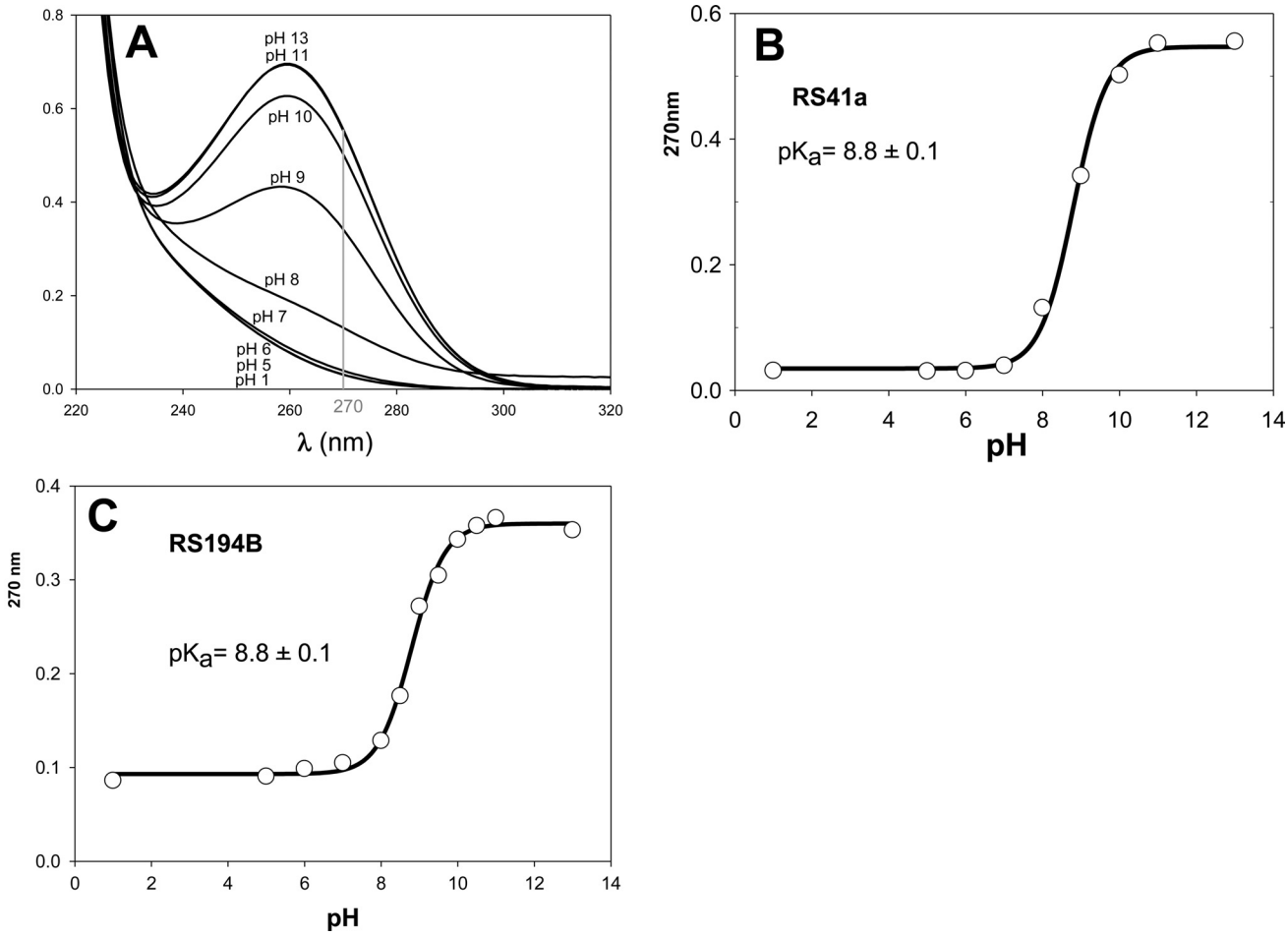

FIGURE 2. **pH dependence of UV spectra of 50 μM RS41A and pH dependence of $A_{270\ nm}$ of 50 μM (*A*) RS41A (*B*), and RS194B along with corresponding pK_a values calculated by nonlinear regression using Equation 1 (*C*).**

TABLE 3

Summary of pK_a values for lead oxime RS194B and other selected oximes determined by four different techniques from pH-dependent changes in oxime UV spectra (*cf.* Fig. 2), oxime ^{1}H NMR spectra in D_2O (*cf.* Fig. 3), oxime-induced ATCh oximolysis (*cf.* supplemental Fig. S3), and oxime-induced VX Flu-MP oximolysis (*cf.* supplemental Fig. S4)

Constants were calculated by nonlinear regression using Equation 1. ND, not determined.

	Oxime pK_a				
			Oximolysis		
Oxime	UV spectra	^{1}H NMR spectra[a]	ATCh	VX Flu-MP	Average pK_a[a]
RS194B	8.8 ± 0.2	9.1 ± 0.1 (-OH) 9.3 ± 0.1 (NH^+)[b] 9.2 ± 0.1 (NH^+)[c]	9.0 ± 0.1	8.9 ± 0.1	8.8 (-OH) 8.8 (NH^+)
RS41A	8.8 ± 0.1	ND	9.0 ± 0.1	8.7 ± 0.1	8.8
RS186B	8.3 ± 0.1	ND	8.5 ± 0.1	ND	8.4
RS150D	ND	ND	10.1 ± 0.1	ND	10.1
RS174C	ND	ND	6.5 ± 0.1	ND	6.5
MINA	8.3 ± 0.1	ND	8.7 ± 0.1	ND	8.5
2PAM	ND	8.6 ± 0.1 (-OH)	8.0 ± 0.1	8.1 ± 0.2	8.1

[a] pK_a values determined in D_2O, as shown, are typically higher than those determined in H_2O by ~0.5 (27) and were corrected before calculating the average pK_a.
[b] Based on pH induced shift of 3.37 ppm triplet in D_2O (Figs. 3*B* and supplemental Fig. S1).
[c] Based on pH induced shift of 3.73 ppm triplet in D_2O (Figs. 3*C* and supplemental Fig. S1).

Pretreatment of mice with RS194B either 5 or 15 min before VX exposure provided notable protection effects only at the highest oxime dose applied (Table 6). However, a combination of 15-min oxime pretreatment and post-VX exposure therapy with 125 mg/kg RS194B produced an exceptionally high protective index of 45 and ensured survival of all mice against VX dose of 31.8 multiples of its LD_{50} that equals 900 μg/kg of VX. Combining pretreatment with therapy enhanced RS194B protective indices, albeit to a smaller extent, also for paraoxon, soman, and tabun (Table 6).

RS41A and RS194B Pharmacokinetics in Mice—Upon i.m. administration of a single dose of 80 mg/kg RS194B or 30 mg/kg RS41A, maximal concentrations determined in plasma were 10 and 27 μg/ml, respectively (equivalent to 54 and 125 μM) observed at the initial collection time point (Fig. 5; supplemental Table S1). The time needed for maximal plasma concentra-

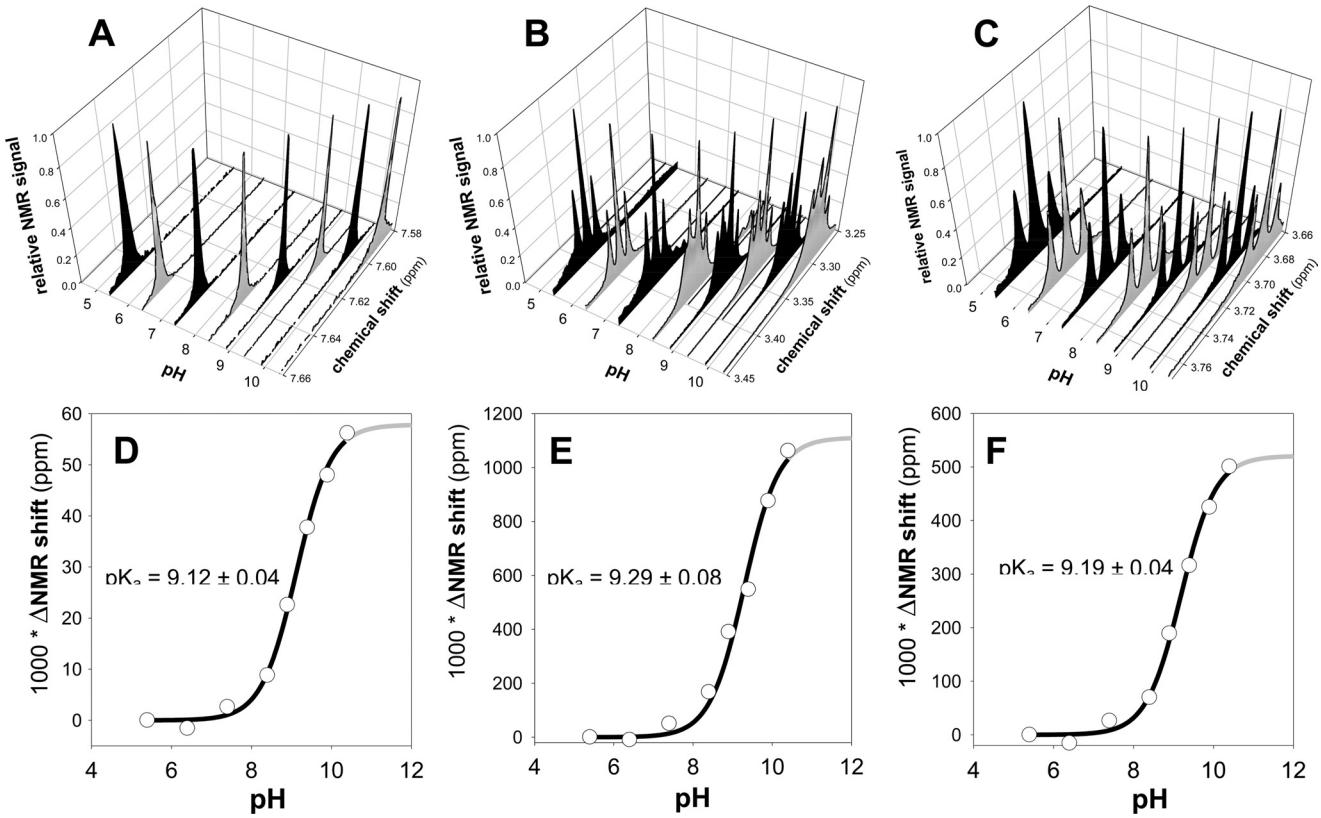

FIGURE 3. **pH dependence of ^{1}H NMR spectra of 2.0 mM RS194B in D_2O buffers (*A*, *B*, and *C*) along with corresponding pK_a values calculated from the observed pH-induced difference in chemical shifts (*D*, *E*, and *F*) by nonlinear regression using Equation 1.** NMR signals in panels *A*, *B*, and *C* were normalized relative to the maximal peak height in the given chemical shift region. Spectra were aligned using a benzene external standard singlet at 7.16 ppm.

TABLE 4

Kinetic constants for reactivation of VX-hAChE conjugate by oximes RS194B, RS41A, RS186B, and reference oxime 2PAM determined in 0.1 M phosphate buffers pH 6.4, 7.4, and 8.4

Oxime	pH	k_2	K_{ox}	k_r
		min^{-1}	mM	$M^{-1}\ min^{-1}$
RS194B	6.4	2.1 ± 0.2	3.2 ± 1.0	620 ± 130
	7.4	3.1 ± 0.1	2.1 ± 0.3	1600 ± 130
	8.4	3.3 ± 0.3	4.2 ± 1.0	790 ± 120
RS41A	6.4	1.4 ± 0.2	3.3 ± 1.4	410 ± 110
	7.4	3.1 ± 0.3	4.6 ± 0.9	670 ± 80
	8.4	3.5 ± 0.3	2.5 ± 0.6	1400 ± 210
2PAM	6.4	0.25 ± 0.01	0.091 ± 0.028	2800 ± 780
	7.4	0.65 ± 0.08	0.25 ± 0.12	2600 ± 910
	8.4	0.80 ± 0.04	0.36 ± 0.08	2200 ± 390
RS186B	6.4	0.23 ± 0.01	3.6 ± 0.7	63 ± 10
	7.4	0.36 ± 0.02	2.7 ± 0.4	130 ± 18
	8.4	0.35 ± 0.02	3.5 ± 0.6	99 ± 15

tions to decay by half was 11 min and 12 min for RS41A and RS194B, respectively. The decay kinetics over this interval likely reflects the distribution into tissue from the plasma as well as total body elimination. The distinctly non-first order elimination of the RS compounds from plasma is consistent with a multicompartmental analysis. Both compounds rapidly penetrated the blood-brain barrier. Maximal brain concentrations determined as 1.2 and 7.9 μg/ml (~6.5 and ~37 μM), respectively, for RS41A and RS194B, reduced in half in 30 and 60 min. RS194B established between 15 and 40 min post-administration an apparent steady state concentration in brain, presumably due to the increased rate of brain accumulation, and plasma declines in concentration (supplemental Table S1).

The resulting brain/plasma ratios at the t_{max} were thus significantly, 2–3-fold higher, for RS194B (0.30) than for RS41A (0.12). Brain levels of both oximes, in particular RS194B, at the final time point (180 min; Fig. 5) were higher than plasma concentrations, suggesting that elimination from this tissue lagged compared with systemic peripheral clearance.

DISCUSSION

The data presented herein are based on our recent revelation that *N*-substituted 2-hydroxyimino acetamidoalkyl amines, although devoid of a permanent cationic charge, can efficiently reactivate OP conjugated hAChE *in vitro* (1). Formation of protonation equilibria around two ionizable groups in those oxime structures, an oxime group and an additional amine group, results in coexistence of charged, zwitterionic, and uncharged reactivator species around physiological pH values. Although zwitterionic and cationic species have the best chance of productive interaction with OP-hAChE conjugates, the uncharged species can be expected to cross the blood-brain barrier delivering reactivator into CNS.

Our starting point for optimization was the structure of initially recognized lead hydroxyiminoacetamido alkylamine reactivator, RS41A. Introduction of systematic structural modifications in both its aliphatic linker and heterocyclic handle led to oxime structures with severalfold improved potency for *in vitro* reactivation of four OP-hAChE conjugates culminating with new lead oxime structure RS194B. Not only were we able to design a more efficient reactivator, but through detailed

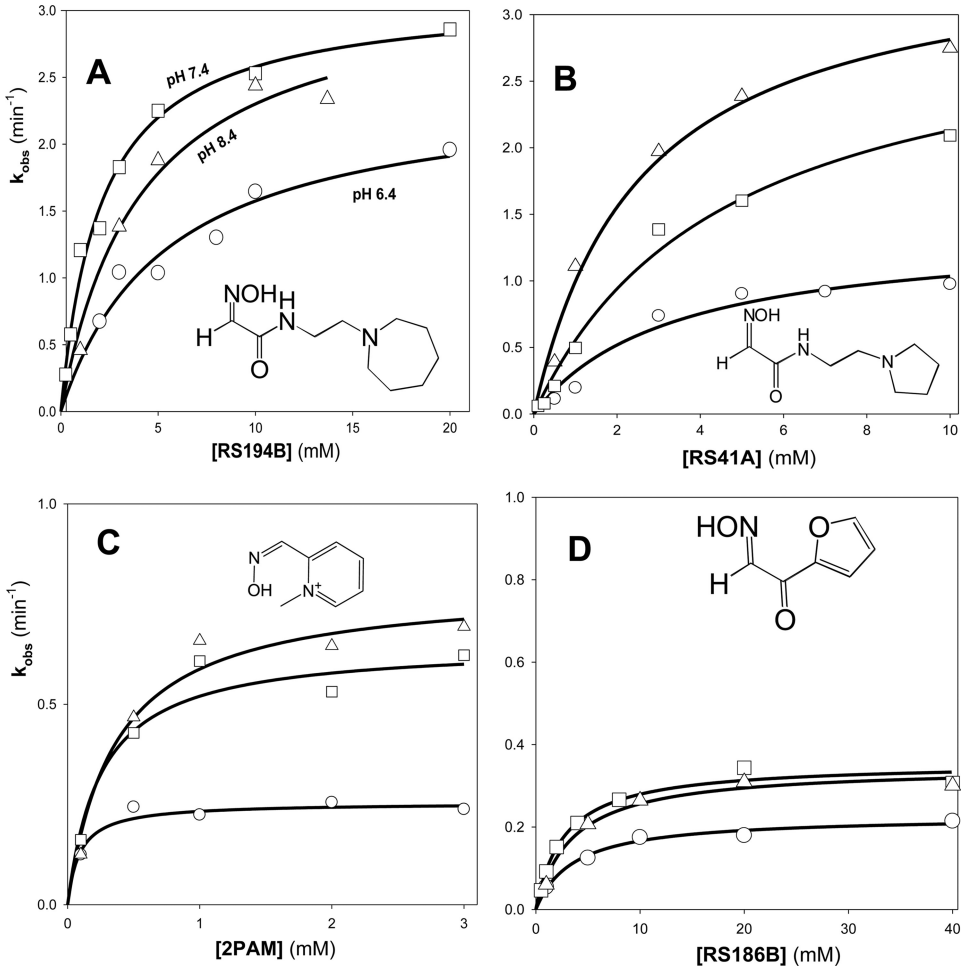

FIGURE 4. **Concentration dependence of oxime reactivation of VX-inhibited hAChE by the lead oxime RS194B (*A*), initial lead oxime RS41A (*B*), and reference oxime 2PAM (*C*) and oxime RS186B (*D*) measured at pH 6. 4 (○), pH 7.4 (□), and pH 8.4 (△) at 37 °C in 0.10 M phosphate buffers.**

TABLE 5

Therapy of OP-exposed mice with lead oximes RS194B and RS41A and standard reference oxime 2PAM. Protective index is the ratio of OP LD_{50} for OP-exposed animals treated with oxime (+atropine) and for animals given OP alone (*cf.* supplemental Tables S2–S6)

95% confidence limits are given in parentheses. ND, not determined.

Oxime	LD_{50}	Dose	Protective index				
			VX	Sarin	Paraoxon	Soman	Tabun
	mg/kg	*mg/kg*					
RS41A	200 (160.9–248.8)	50	4.5 (3.8–5.3)	<1 (ND)	<1 (ND)	1.3 (1.1–1.5)	1.2 (1.0–1.4)
RS194B	500[a]	125	18 (12.4–25.7)	10 (6.6–15.3)	9.4 (7.9–11.3)	1.8 (1.5–2.1)	1.5 (1.2–1.7)
2PAM	106 (94.0–118.4)	26.4	9.3 (7.3–13.0)	6.7 (5.9–7.5)	47 (36.7–59.5)	1.5 (1.3–1.8)	1.3 (1.1–1.5)

[a] Estimated from 50% lethality at the maximal administered dose due to solubility limitations.

analysis of reactivation kinetics, we obtained insights into regulatory structural constraints imposed by varying geometries of OP-hAChE conjugates. Reversible binding of a reactivator leading to progressive reactivation is thus facilitated by propyl linker and a bridged azepane heterocycle, whereas optimal geometry of AChE-OP-oxime trigonal bipyramidal intermediate is achieved with ethyl linker. The greater *in vitro* reactivation rate of RS194B is, therefore, largely a reflection of its improved molecular recognition, *i.e.* better binding to OP-hAChE conjugates as indicated by smaller K_{ox} constants while maintaining similar k_2 constants, in comparison to RS41A. This effectively means that improved oxime·OP-hAChE interactions in the reversible complex were also preserved in the subsequent reaction trigonal bipyramidal intermediate. Computational molecular modeling of two reaction steps for RS41A and RS194B oximes consistently reveals more pronounced similarity in geometries of reversible complex and trigonal bipyramidal intermediate for RS194B oxime and not with RS41A oxime (Fig. 6). Additionally, modeling suggests that the main anchoring point of both RS41A and RS194B oximes in interaction with VX-hAChE is the aromatic amino acid cluster of the AChE peripheral site.

Analysis of ionization states of RS194B by UV spectroscopy, ^{1}H NMR spectrometry, and pH dependence of oximolysis reveals that both oxime group and amino group in the reactivator handle have pK_a constants in the range between 8.6 and 9.0. At physiological pH 7.4, therefore, more than 90% of the compound exists in the protonated, cationic form. That seems

TABLE 6

Combination of therapy and pretreatment of OP-exposed mice with oxime RS194B at doses equivalent to 25, 10, or 5% its LD_{50} dose of 500 mg/kg (*cf.* supplemental Tables S2–S6)

Protective index is the ratio of OP LD_{50} for OP-exposed animals treated with oxime and for animals given OP alone. Maximal dose of poison (MDP), a highest multiple of OP LD_{50} fully counteracted by the oxime, is given in parentheses. Oximes in therapy (but not in pretreatment) were administered together with atropine. ND, not determined.

	Protective index (MDP) (95% confidence limits)			
	Pretreatment before VX			
RS194B	5 min	15 min	Therapy 1 min after VX	Pretreatment 15 min and therapy 1 min after VX
25 mg/kg	2.0 (1.6) (1.8–2.3)	1.6 (ND) (1.2–2.1)	5.3 (4) (4.8–6.0)	
50 mg/kg		1.3 (1.0) (1.1–1.6)	11 (7.9) (8.5–13.7)	7.3 (5.0) (5.6–9.6)
125 mg/kg	3.7 (2.5) (2.9–4.7)	3.6 (2.5) (3.0–4.2)	18 (10.0) (12.4–25.7)	45 (31.8) (37.2–54.3)
	Pretreatment 15 min and therapy 1 min after OP			
	Paraoxon	Soman	Tabun	Sarin
125 mg/kg	22 (7.9) (17.0–27.5)	2.8 (2.5) (ND)	2.0 (ND) (1.3–3.1)	4.5 (3.2) (3.8–5.3)

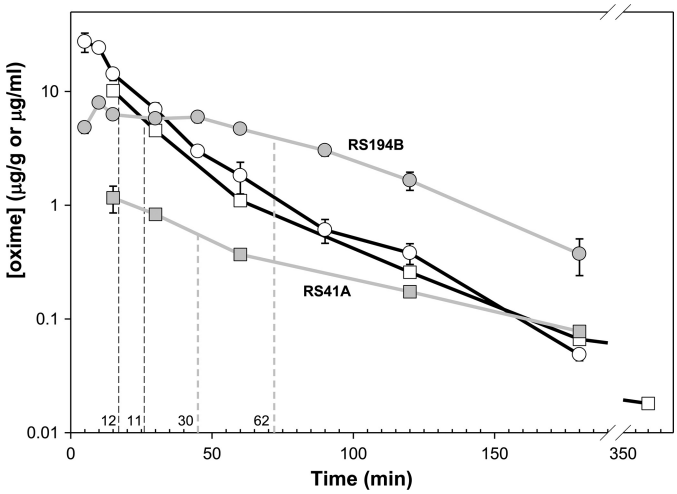

FIGURE 5. **Pharmacokinetics of RS194B (*circles*) and RS41A (*squares*) in mice. Brain (*gray lines*) and plasma (*black lines*) compound concentrations were determined at discrete time points upon single, 80 mg/kg (RS194B), or 30 mg/kg (RS41A) dose administered to mice i.m.** Each point represents average of determinations from three mice. S.E. of determination are indicated by *error bars*. Times required for halving maximal compound concentrations in plasma and in brain are indicated by *dashed lines* for each of two oximes.

to be reflected in reasonable *in vitro* reactivation kinetics where the initial reversible binding is improved for RS194B *versus* RS41A (lower K_{ox}) while maintaining respectable reactivity (a small decrease in k_2). A low fraction of oximate is thus counteracted by high nucleophilicity (supplemental Fig. S3) and preferred for CNS reactivators due to lower ionization of the oximate facilitating blood brain barrier penetration.

Despite the suggestion that reactivators with lower oxime pK_a may be intrinsically more reactive at physiological pH in the absence of enzyme (Fig. 7 and Ref. 26), their overall reactivation potency expressed by constant k_r was not found to correlate closely with the oximate pK_a (in the wide pK_a range 6.5–10.1) for reactivation of any of OP-hAChE conjugates analyzed individually (supplemental Fig. S5) or as an average (Fig. 7). The linear increase of the maximal rate of reactivation log k_2 with the increase in pK_a, observed for five studied reactivators (supplemental Fig. S6*E*), however, reveals a greater dependence of reactivator nucleophilic strength for reactivity of AChE-OP-oxime trigonal bipyramidal intermediate when compared with fractional availability of oximate anion at physiological pH determined by the oximate pK_a. This observation may indicate an effective proton extraction mechanism for oxime reactions in the hAChE active center gorge. On the other hand domination of the protonated amine at pH 7.4 influences the capacity of RS194B to enter the CNS. Nevertheless, pharmacokinetic studies in mice indicate that both RS194B and RS41A oximes penetrate CNS quickly and can be found there at up to 37 and 6.5 μM concentrations, which are ~12–30% of corresponding plasma concentrations.

Very good antidotal actions of RS194B in treatment of OP exposed mice relative to RS41A or 2PAM treatments undoubtedly result from its improved intrinsic reactivation potency combined with its lower toxicity and superior pharmacokinetic profile including faster CNS penetration and longer retention. However, a favorable antidotal action of RS194B was noticeable even at doses equivalent to 5 and 10% its LD_{50} value. RS194B was most efficient in therapy of VX, sarin, and paraoxon exposed mice, where it was superior to both RS41A and to a standard reactivator 2PAM (except for paraoxon intoxication). Although RS194B, when given solely as a pretreatment modality, produced limited prophylactic protection to subsequent OP exposure, consistent with its relatively low binding affinity for AChE conjugates (large K_{ox} values), the combination of pretreatment and therapy at the highest RS194B dose resulted in outstanding antidotal efficiency reflected in the protective index of 45.

Several classes of novel compounds have been recently suggested as promising centrally active reactivators of OP-exposed hAChE. Two nonquaternary pyridine aldoxime phenyltetrahydroisoquinoline derivatives directed to interact with the AChE peripheral site showed outstanding potency for *in vitro* reactivation of VX and tabun-conjugated hAChE (2). Thus, uncharged, extended ligands with high affinities for the peripheral site form an alternative means of directing nucleophiles to the organophosphate conjugated active center (28). The overall second order rate constant (k_r) for reactivation of VX-hAChE conjugate by phenyltetrahydroisoquinoline derivatives was an

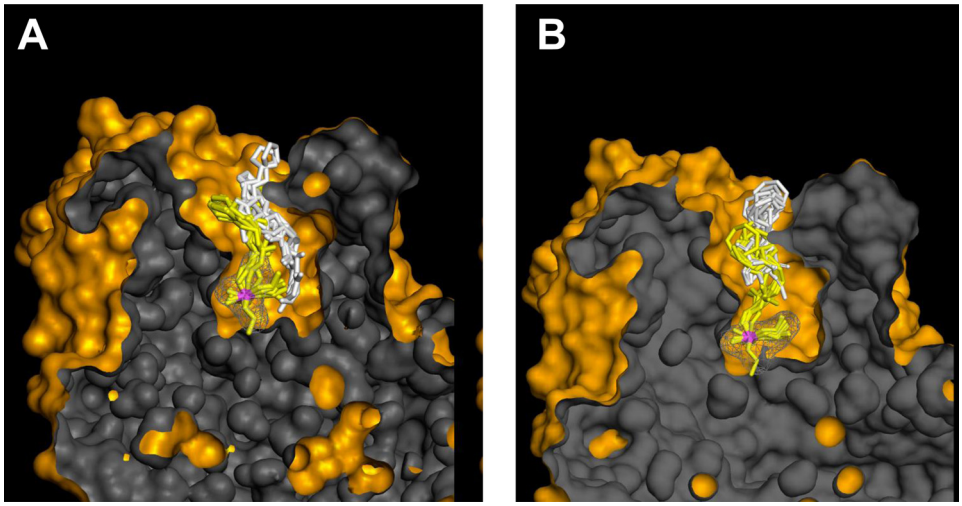

FIGURE 6. **Computational molecular modeling of VX-inhibited AChE showing the reversible Michaelis type complex (*white sticks*) and covalent pentacoordinate trigonal bipyramidal intermediate (*yellow sticks*) for interaction of initial lead oxime RS41A (*A*) and the lead oxime RS194B (*B*).** Ten conformers of each oxime are shown in each of two interaction states. The phosphorus atom is colored *purple*. The solvent-accessible part of the hAChE Connolly surface is represented in *orange*, and the solvent-inaccessible part of the hAChE molecule is in *dark gray*. Pronounced overlapping similarity in global geometries of the reversible complex (*white sticks*) and trigonal bipyramidal intermediate (*yellow sticks*) was observed for RS194B oxime, but not with RS41A oxime.

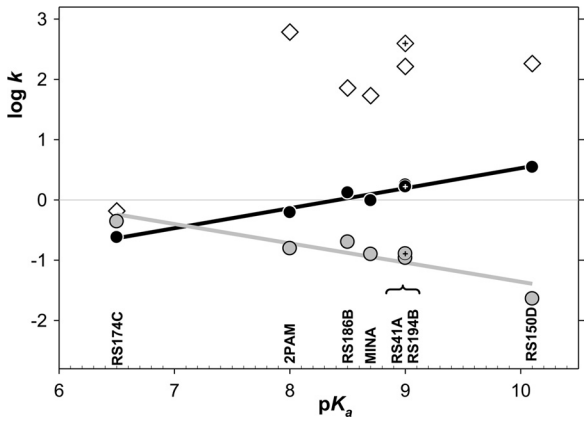

FIGURE 7. **Free energy relationships between nucleophilic reactivities and oxime group ionization states of selected oxime reactivators.** Rate constants (k) of maximal pH-dependent ATCh oximolysis (*black line* and *circles*), oximolysis at pH 7.4 (*gray line* and *circles*), and an average overall rate constant k_r ($M^{-1}min^{-1}$) for oxime reactivation of VX, sarin, cyclosarin, and paraoxon inhibited hAChE (*white diamonds*) in relation to pK_a values were determined for reactivator oxime groups. The lead reactivator RS194B data is indicated by cross-haired symbols. k_r for RS174C and RS150D (not extensively studied in this series) were extrapolated from reactivation rates determined at single (0.67 mM) oxime concentration.

order of magnitude larger than the corresponding RS194B constant despite nearly an order of magnitude smaller maximal reactivation rate constant (k_2) and largely due to their high apparent affinity for VX-hAChE conjugate ($K_{ox} = 6-47\ \mu M$). However, these compounds lack pharmacokinetic, toxicity, and efficacy analyses.

A similar series of α-ketoaldoxime derivatives of polycyclic peripheral site-directed ligands also exhibited initial promise in reactivation of VX and sarin-conjugated hAChE, whereas tabun-hAChE conjugate reactivation was less efficient (3). Finally, several amidine-based oximes indicated positive *in vitro* and *in vivo* initial properties for reactivation of hAChE inhibited by charged or less volatile nerve agent analogues (4). Although *in vitro* reactivation approached 2PAM reactivation levels, *in vivo* efficacy for treatment of nerve agent-exposed mice is difficult to assess as low toxicity nerve agent surrogates were used as toxicants.

In summary, this study presents uniquely comprehensive characterization of a novel series of *N*-substituted 2-hydroxyimino acetamido alkylamine reactivators of nerve agent-conjugated hAChE. Through systematic steps of structural modifications, we refined the initial lead RS41A into a superior RS194B reactivator of VX-, sarin-, paraoxon-, cyclosarin-, and tabun-conjugated hAChE both *in vitro* and *in vivo*. Cyclosarin has yet to be tested *in vivo*. Outstanding intrinsic reactivation potencies of this oxime, resulting in part from its favorable interaction with the peripheral site of AChE, in combination with its low toxicity results provide the lead for a pan-reactive antidote for the treatment of OP-exposed mice, either post-exposure or in combination of prophylactic and antidotal oxime treatments of OP-exposed animals.

Acknowledgments—The assistance of Jasna Mileković with the in vivo therapeutic study and Dr. Brendan Duggan with recording two-dimensional $^1H,^1H$ double-quantum filtered COSY NMR spectra was greatly appreciated.

REFERENCES

1. Sit, R. K., Radić, Z., Gerardi, V., Zhang, L., Garcia, E., Katalinić, M., Amitai, G., Kovarik, Z., Fokin, V. V., Sharpless, K. B., and Taylor, P. (2011) New structural scaffolds for centrally acting oxime reactivators of phosphylated cholinesterases. *J. Biol. Chem.* **286,** 19422–19430
2. Mercey, G., Verdelet, T., Saint-André, G., Gillon, E., Wagner, A., Baati, R., Jean, L., Nachon, F., and Renard, P. Y. (2011) First efficient uncharged reactivators for the dephosphylation of poisoned human acetylcholinesterase. *Chem. Commun.* **475,** 5295–5297
3. de Koning, M. C., van Grol, M., and Noort, D. (2011) Peripheral site ligand conjugation to a non-quaternary oxime enhances reactivation of nerve agent-inhibited human acetylcholinesterase. *Toxicol. Lett.* **206,** 54–59
4. Kalisiak, J., Ralph, E. C., Zhang, J., and Cashman, J. R. (2011) Amidine-oximes. Reactivators for organophosphate exposure. *J. Med Chem.* **54,** 3319–3330
5. Demar, J. C., Clarkson, E. D., Ratcliffe, R. H., Campbell, A. J., Thangavelu,

S. G., Herdman, C. A., Leader, H., Schulz, S. M., Marek, E., Medynets, M. A., Ku, T. C., Evans, S. A., Khan, F. A., Owens, R. R., Nambiar, M. P., and Gordon, R. K. (2010) Pro-2-PAM therapy for central and peripheral cholinesterases. *Chem. Biol. Interact.* **187,** 191–198
6. Garcia, G. E., Campbell, A. J., Olson, J., Moorad-Doctor, D., and Morthole, V. I. (2010) Novel oximes as blood-brain barrier penetrating cholinesterase reactivators. *Chem. Biol. Interact.* **187,** 199–206
7. Little, P. J., Scimeca, J. A., and Martin, B. R. (1988) Distribution of [^{3}H]diisopropylfluorophosphate, [^{3}H]soman, [^{3}H]sarin and their metabolites in mouse brain. *Drug Metab. Dispos.* **16,** 515–520
8. Wilson, I. B., and Bergmann, F. (1950) Studies on cholinesterase. VII. The active surface of acetylcholine esterase derived from effects of pH on inhibitors. *J. Biol. Chem.* **185,** 479–489
9. Aldridge, W. N., and Reiner, E. (1972) *Enzyme Inhibitors as Substrates*, North Holland, Amsterdam
10. Sussman, J.L., Harel, M., Frolow, F., Oefner, C., Goldman, A., Toker, L., and Silman, I. (1991) Atomic structure of acetylcholinesterase from *Torpedo californica*. A prototypic acetylcholine-binding protein. *Science* **253,** 872–879
11. Harel, M., Schalk, I., Ehret-Sabatier, L., Bouet, F., Goeldner, M., Hirth, C., Axelsen, P.H., Silman, I., and Sussman, J.L. (1993) Quaternary ligand binding to aromatic residues in the active site gorge of acetylcholinesterase. *Proc. Natl. Acad. Sci. U.S.A.* **90,** 9031–9035
12. Lewis, W. G., Green, L. G., Grynszpan, F., Radić, Z., Carlier, P. R., Taylor, P., Finn, M. G., and Sharpless, K. B. (2002) Click chemistry *in situ*. Acetylcholinesterase as a reaction vessel for the selective assembly of a femtomolar inhibitor from an array of building blocks. *Angew. Chem. Int. Ed. Engl.* **41,** 1053–1057
13. Radić, Z., and Taylor, P. (2006) in *Toxicology of Organophosphate and Carbamate Compounds* (Gupta, R., ed) pp. 161–186, Elsevier, Amsterdam
14. Silman, I., and Sussman, J. L. (2008) Acetylcholinesterase. How is structure related to function? *Chem. Biol. Interact.* **175,** 3–10
15. Shih, T. M., Skovira, J. W., O'Donnell, J. C., and McDonough, J. H. (2010) *In vivo* reactivation by oximes of inhibited blood, brain, and peripheral tissue cholinesterase activity after exposure to nerve agents in guinea pigs. *Chem. Biol. Interact.* **187,** 207–214
16. Cochran, R., Kalisiak, J., Küçükkilinç, T., Radic, Z., Garcia, E., Zhang, L., Ho, K. Y., Amitai, G., Kovarik, Z., Fokin, V. V., Sharpless, K. B., and Taylor, P. (2011) Oxime-assisted acetylcholinesterase catalytic scavengers of organophosphates that resist aging. *J. Biol. Chem.* **286,** 29718–29724
17. Amitai, G., Adani, R., Yacov, G., Yishay, S., Teitlboim, S., Tveria, L., Limanovich, O., Kushnir, M., and Meshulam, H. (2007) Asymmetric fluorogenic organophosphates for the development of active organophosphate hydrolases with reversed stereoselectivity. *Toxicology* **233,** 187–198
18. Ellman, G. L., Courtney, K. D., Andres V., Jr., and Feather-Stone, R. M. (1961) A new and rapid colorimetric determination of acetylcholinesterase activity. *Biochem. Pharmacol.* **7,** 88–95
19. Kovarik, Z., Radić, Z., Berman, H.A., Simeon-Rudolf, V., Reiner, E., and Taylor, P. (2004) Mutant cholinesterases possessing enhanced capacity for reactivation of their phosphonylated conjugates. *Biochemistry* **43,** 3222–3229
20. Malany, S., Sawai, M., Sikorski, R. S., Seravalli, J., Quinn, D. M., Radić, Z., Taylor, P., Kronman, C., Velan, B., and Shafferman, A. (2000) Transition state structure and rate determination for the acylation stage of acetylcholinesterase-catalyzed hydrolysis of (acetylthio)choline. *J. Am. Chem. Soc.* **122,** 2981–2987
21. Ashani, Y., Radić, Z., Tsigelny, I., Vellom, D. C., Pickering, N. A., Quinn, D. M., Doctor, B. P., and Taylor, P. (1995) Amino acid residues controlling reactivation of organophosphonyl conjugates of acetylcholinesterase by mono- and bisquaternary oximes. *J. Biol. Chem.* **270,** 6370–6380
22. Thompson, W. R. (1947) Use of moving averages and interpolation to estimate median-effective dose. *Bacteriol. Rev.* **11,** 115–145
23. Weil, C. S. (1952) Tables for convenient calculation of median-efffective dose (LD_{50} or ED_{50}) and instruction in their use. *Biometrics* **8,** 249–263
24. Čalić, M., Vrdoljak, A. L., Radić, B., Jelić, D., Jun, D., Kuca, K., and Kovarik, Z. (2006) *In vitro* and *in vivo* evaluation of pyridinium oximes. Mode of interaction with acetylcholinesterase, effect on tabun- and soman-poisoned mice and their cytotoxicity. *Toxicology* **219,** 85–96
25. Berend, S., Katalinić, M., Vrdoljak, A. L., Kovarik, Z., Kuca, K., and Radić, B. (2010) *In vivo* experimental approach to treatment against tabun poisoning. *J. Enzyme Inhib. Med. Chem.* **25,** 531–536
26. Wilson, I. B., and Froede, H. C. (1971) in *Drug Design* (Ariens, E. J., ed) Vol. II, pp. 213–229, Academic Press, New York
27. Cook, P. F., and Cleland, W. W. (2007) *Enzyme Kinetics and Mechanism*, pp. 225–368, Garland Science, London
28. Krasiński, A., Radić, Z., Manetsch, R., Raushel, J., Taylor, P., Sharpless, K.B., and Kolb, H.C. (2005) In situ selection of lead compounds by click chemistry: target-guided optimization of acetylcholinesterase inhibitors. *J. Am. Chem. Soc.* **127,** 6686–6692